Barium uptake into the shells of the common mussel (*Mytilus edulis*) and the potential for estuarine paleo-chemistry reconstruction

David P. Gillikin [a,*], Frank Dehairs [a], Anne Lorrain [b,1], Dirk Steenmans [a], Willy Baeyens [a], Luc André [b]

[a] *Department of Analytical and Environmental Chemistry, Vrije Universiteit Brussel, Pleinlaan 2, B-1050 Brussels, Belgium*
[b] *Section of Mineralogy and Petrography, Royal Museum for Central Africa, Leuvensesteenweg 13, B-3080 Tervuren, Belgium*

Abstract

In this study we test if calcite shells of the common mussel, *Mytilus edulis*, contain barium in proportion to the water in which they grew. Similar to all bivalves analyzed to date, the $[Ba/Ca]_{shell}$ profiles are characterized by a relatively flat background $[Ba/Ca]_{shell}$, interrupted by sharp $[Ba/Ca]_{shell}$ peaks. Previous studies have focused on these $[Ba/Ca]_{shell}$ peaks, but not on the background $[Ba/Ca]_{shell}$. We show that in both laboratory and field experiments, there is a direct relationship between the background $[Ba/Ca]_{shell}$ and $[Ba/Ca]_{water}$ in *M. edulis* shells. The laboratory and field data provided background Ba/Ca partition coefficients (D_{Ba}) of 0.10 ± 0.02 and 0.071 ± 0.001, respectively. This range is slightly higher than the D_{Ba} previously determined for inorganic calcite, and slightly lower than foraminiferal calcite. These data suggest that *M. edulis* shells can be used as an indicator of $[Ba/Ca]_{water}$, and therefore, fossil or archaeological *M. edulis* shells could be used to extend knowledge of estuarine dissolved Ba throughputs back in time. Moreover, considering the inverse relationship between $[Ba/Ca]_{water}$ and salinity, background $[Ba/Ca]_{shell}$ data could be used as an estuary specific indicator of salinity. The cause of the $[Ba/Ca]_{shell}$ peaks is more confusing, both the laboratory and field experiments indicate that they cannot be used as a direct proxy of $[Ba/Ca]_{water}$ or phytoplankton production, but may possibly be caused by barite ingestion.
© 2005 Elsevier Inc. All rights reserved.

1. Introduction

In recent years there has been an increasing amount of papers presenting high resolution elemental profiles in bivalve shells. Unlike corals and foraminifera, much of the bivalve data presented suggests that many of these elemental profiles (e.g., Sr, Mn, Pb, U), which often largely differ from expected concentrations based on inorganic and other biogenic carbonates, cannot be used as proxies of environmental conditions (e.g., Stecher et al., 1996; Purton et al., 1999; Vander Putten et al., 2000; Takesue and van Geen, 2004; Freitas et al., 2005; Gillikin et al., 2005a; Gillikin, 2005). There have been some promising reports of bivalve shell Mg/Ca ratios as a proxy of sea surface temperature (SST) (Klein et al., 1996), but other reports illustrate that this is not always the case, and is apparently strongly species specific (Vander Putten et al., 2000; Takesue and van Geen, 2004; Freitas et al., 2005; Gillikin, 2005; Lorrain et al., 2005). Bivalve shell Ba/Ca ratios on the other hand have been shown to be highly reproducible between specimens and have been hypothesized to be a proxy of both particulate Ba (Stecher et al., 1996; Vander Putten et al., 2000; Lazareth et al., 2003) and dissolved Ba (Torres et al., 2001), and therefore could be particularly promising.

The oceanic barium cycle has received much attention over the past several decades (e.g., Chan et al., 1977;

---

* Corresponding author. Fax: +32 2 629 3274.

E-mail addresses: david.gillikin@vub.ac.be, david@scientificproofreading.com (D.P. Gillikin).

[1] Present address: UR Thetis, IRD-CRH (Centre de Recherche Halieutique Méditerranéenne et Tropicale), Avenue Jean Monnet-BP 171, 34203 Sète Cedex, France.

Dehairs et al., 1980, 1992; Paytan and Kastner, 1996; McManus et al., 2002; Jacquet et al., 2005). This is due in part to the use of Ba as a paleoproductivity and paleo-alkalinity proxy (Dymond et al., 1992; Lea, 1993; McManus et al., 1999). Barium enters the oceans from river or ground water inputs, which pass through estuaries and the coastal zone (Carroll et al., 1993; Guay and Falkner, 1997; Guay and Falkner, 1998; Shaw et al., 1998). Obtaining insight into the magnitude and temporal variability of these Ba inputs is important for understanding the oceanic Ba cycle and residence time, as shown by many studies (Edmond et al., 1978; Moore and Edmond, 1984; Coffey et al., 1997; Guay and Falkner, 1997, 1998); however, historical records of riverine inputs are lacking. Having a proxy of Ba inputs from estuaries or the coastal zone that can be extended back in time would be highly valuable.

Barium/calcium ratios have been proposed as a proxy of dissolved seawater Ba/Ca in aragonitic corals (Tudhope et al., 1996; McCulloch et al., 2003; Sinclair and McCulloch, 2004), calcitic foraminifera (Lea and Boyle, 1989, 1991) and vesicomyid clam shells (Torres et al., 2001), providing information on salinity, nutrient and alkalinity distributions in past oceans.

To date, all published records of high resolution Ba profiles in bivalve shells (both aragonite and calcite) have similar characteristics with a more or less stable background Ba concentration, interspaced with sharp episodic Ba peaks (Stecher et al., 1996; Toland et al., 2000; Vander Putten et al., 2000; Torres et al., 2001; Lazareth et al., 2003; Gillikin, 2005). Stecher et al. (1996) first proposed that these peaks were the result of the filter feeding bivalves ingesting Ba-rich particles associated with diatom blooms, as either phytoplankton, or barite. It is well known that primary productivity and barite formation are closely associated (e.g., Dehairs et al., 1980, 1987). Once inside the digestive tract, Ba may be metabolized and moved via the hemolymph to the extrapallial fluid (EPF), where shell precipitation occurs (Wilbur and Saleuddin, 1983). Vander Putten et al. (2000) found a remarkable coincidence of the Ba peaks in several mussel shells collected at the same site, providing further evidence that an environmental parameter controls their occurrence. However, this hypothesis remains untested. Furthermore, there are no studies reporting the Ba/Ca partition coefficient ($D_{Ba} = (Ba/Ca)_{carbonate}/(Ba/Ca)_{water}$) for bivalves and the only study suggesting that bivalves record dissolved Ba may possibly have included the effects of these shell Ba peaks (see Torres et al., 2001). Rosenthal and Katz (1989) found a good correlation between dissolved Ba/Ca and shell Ba/Ca in two species of freshwater aragonitic gastropods, but analyzed large shell sections and may have also included shell Ba/Ca peaks.

The aim of this study was to assess if calcite shells of the common mussel, *Mytilus edulis*, contain barium in proportion to the water in which they grew. To validate this proxy, we measured Ba concentrations in the shells, soft tissues and hemolymph of mussels exposed to different levels of dissolved Ba in the laboratory as well as mussels fed diets with varying Ba concentrations. To calibrate the proxy on natural populations, a field study along the Westerschelde Estuary (The Netherlands) was conducted, where mussels were grown along a salinity gradient while elemental concentrations and physico-chemical water parameters were regularly monitored. This experimental setup allowed us to compare data from both culture and natural situations.

2. Materials and methods

2.1. Laboratory experiments

2.1.1. Dissolved Ba experiment

Mytilus edulis were collected from the Oosterschelde estuary near Wemeldinge, The Netherlands (salinity ~35; temperature ~8 °C) on 1 March 2004 (Fig. 1). Epibionts were gently removed and the mussels were acclimated to laboratory conditions at 9.2 ± 0.3 °C (mean ± standard deviation) for 7 days, then another 14 days at 14.7 ± 0.2 °C (i.e., 21 days acclimation; temperature monitored hourly with a TidBit data logger, Onset Computer). During acclimation, mussels were fed three times per week with 12 mg of dried yeast per animal per week (Artemic Systems, LANSY PZ). After the acclimation period, 40 mussels (2.8 ± 0.3 cm length) were selected for the 'dissolved Ba' experiment and were stained with calcein (200 mg/L; $C_{30}H_{26}N_2O_{13}$; Sigmal Chemical) for 20 h to mark the beginning of the experiment in the shell (see Rowley and Mackinnon, 1995). Afterwards, 10 mussels were placed in each of four aquaria containing 10 L of filtered (10 μm) North Sea water spiked with approximately 0, 110, 220, and 440 nmol/L of Ba (as $BaCl_2$) (Table 1). Water was continuously circulated through acid washed plastic filters (except during feeding periods, see further) and was aerated. Mussels were fed the same quantities of yeast as during the acclimation period. Feeding took place for 3 h, three times per week. Mussels were fed in their separate aquaria during which the filtration pumps were turned off. This experiment ran for 36 days, during which the water in all tanks was changed weekly (similar to Lorens and Bender, 1980) and was maintained at 16.4 ± 0.6 °C with a pH of 7.9 ± 0.1 and salinity of 36.4 ± 0.9 (on occasion salinity was adjusted with deionized water (>18 MΩ/cm) to compensate for evaporation; pH and salinity were measured with a WTW multiline P4 multimeter). Water samples were taken two times per week for $[Ba/Ca]_{water}$ using syringe filters (Macherey-Nagel; Chromafil A45/25; cellulose mixed esters; 0.45 μm pore size), once just before and after a water change, and were acidified with trace metal grade HCl to ~pH 3. Procedural blanks were also taken by filtering deionized water (>18 MΩ/cm).

2.1.2. Feeding experiment

To assess the effect of Ba being ingested as food, a feeding experiment was conducted. In a fifth aquarium, two plastic mesh baskets, each with 10 mussels were held under
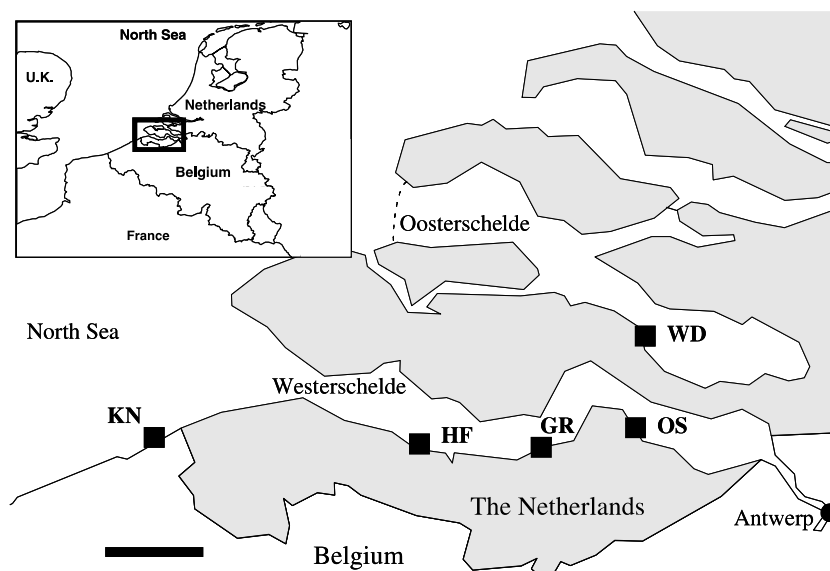
Fig. 1. Map of the Westerschelde and Oosterschelde estuaries. The mussel collection site at Wemeldinge (WD) and the four study sites are indicated: Knokke (KN), Hooftplaat (HF), Griete (GR), and Ossenisse (OS). Scale bar = 10 km.

Table 1
Summary of average seawater $[Ba/Ca]_{water}$ ($\pm$SE) for each laboratory $[Ba/Ca]_{water}$ treatment group

Tank	Treatment[a]	$[Ba/Ca]_{water}$ (μmol/mol)
1	Ambient	5.08 ± 0.22
2	+110 nmol/L	19.38 ± 0.71
3	+220 nmol/L	36.34 ± 0.91
4	+440 nmol/L	65.05 ± 2.37
5	Feeding[a]	4.61 ± 0.45

$N = 8$ water samples per treatment, spread over the experiment.
[a] See text.

the same conditions, except that there was 20 L of water to compensate for the higher density of animals and they were fed differently. These mussels were fed in separate aquaria with different foods. One batch was fed a slurry of living phytoplankton (*Chlamidomonas reinhardii*) grown in a 'normal' Tris-acetate-phosphate (TAP) medium (hereafter referred to as phyto +0) with the phytoplankton containing 5.87 ± 0.51 nmol/g dry weight (DW) Ba ($n = 3$), whereas the other batch were fed the same phytoplankton species, which were grown in a Ba rich TAP medium (spiked with 730 nmol/L Ba; hereafter referred to as phyto +100; see Steenmans (2004) for more details regarding phytoplankton culturing) with $[Ba] = 14.56 \pm 0.95$ nmol/g DW ($n = 3$). Both batches were fed for 1 h per day, 5 days per week, with a total of 18 mg phytoplankton (DW) per animal per week. This provided three levels of Ba in food given to mussels maintained in normal seawater Ba concentrations (i.e., yeast (with $[Ba] = 3.35 \pm 0.32$ nmol/g DW ($n = 3$)), phyto +0 and phyto +100). After feeding, mussels were returned to their aquarium. This experiment was run for 29 days; water maintenance and sampling was similar to the dissolved Ba experiment. Mussels were sampled (7 per treatment) approximately 24 h after the last feeding period. *M. edulis* hemolymph has been determined

to have a slow turnover time based on the residence time (>3 days) of a fluorescent dye (Gillikin, 2005). Therefore, this sampling design should have captured any Ba entering the hemolymph from the food.

2.1.3. Hemolymph, soft tissue, and shell sampling

After the experiments were complete, mussels were removed from their aquaria one at a time and hemolymph, soft tissues, and shells were sampled. Hemolymph was sampled by blotting the shell dry, and then gently prying open the valves with a scalpel, draining the mantle cavity and then sampling the hemolymph from the adductor muscle with a sterile 5 ml syringe and needle. Procedural blanks were prepared by drawing deionized water into a new syringe. Whole tissues were dissected from the valves using a scalpel. Samples (hemolymph and tissues) and blanks were transferred to micro-centrifuge tubes and were immediately frozen to $-20\,^{\circ}$C until analysis. Shells were rinsed with deionized water (>18 MΩ/cm) and were air dried.

A condition index was used to compare mussel health at the end of the experiments ([shell length/shell width]/tissue dry weight) to mussels health at the end of the acclimation period (beginning of experiments), which indicated that all animals were healthy (ANOVA, LSD test, $p > 0.05$ for all).

2.2. Field experiment

Mytilus edulis ($\sim$3 cm) were collected from the Oosterschelde (The Netherlands; Fig. 1). The Oosterschelde estuary was dammed in the late 1980s and now has more or less marine salinities ($S > 30$; Gerringa et al., 1998). Mussels were transported back to the laboratory where epibionts were removed. They were then stained with calcein as in the previously described experiments. Within the next week (on 24 October 2001), 50 mussels were placed into four

stainless steel cages and these were deployed along an estuarine salinity gradient in the Westerschelde estuary (Fig. 1; see Baeyens et al., 1998 for a general description of the Westerschelde). Cages were attached at the same tidal level as the highest density of 'local' mussels at Ossenisse (OS; the most upstream occurrence of wild *Mytilus* populations), Griete (GR), Hooftplaat (HF), and Knokke (KN; Fig. 1). Water temperature was monitored at each site hourly using a TidBit data logger. Near-shore water was sampled monthly at high tide for one year (November 2001–2002) and every 2 weeks between March and May for salinity, dissolved Ba/Ca, and chlorophyll a (Chl a). Salinity was measured in situ with a WTW multiline P4 multimeter. [Ba/Ca]$_{water}$ was sampled by filtering 250–500 ml of seawater through 0.4 µm polycarbonate filters (Osmonics poretics). The filtrate was acidified with trace metal grade HNO$_3$ to ~pH 3. Blanks were prepared by filtering deionized water (>18 MΩ/cm) through the same system and blank filter. Phytoplankton pigments were sampled by filtering 200–500 ml of seawater through Whatman GF-F filters (nominal porosity = 0.7 µm). Filters were wrapped in aluminum foil and placed in liquid nitrogen; three replicates were taken at each sampling. Upon return to the laboratory, samples were transferred to a −85 °C freezer until analysis.

Mussels were collected on four different dates (29 September '02, 9 December '02, 20 February '03, and 21 April '03). Mussels transplanted to OS did not survive (undoubtedly due to the salinity shock) and therefore local mussels from this site were used. Similarly, the wave action at KN repeatedly destroyed cages and all mussels were lost; so again at this site, mussels from the local population were used.

2.3. Sample preparation and analysis

All water samples for dissolved Ba and Ca analysis were diluted with deionized water (>18 MΩ/cm) to assure a salt concentration less than 0.2%. Ba was measured on a VG PlasmaQuad II+ inductively coupled plasma mass spectrometer (ICP-MS) using In as an internal standard. Calcium was measured with an IRIS Thermo Jarrell Ash. ICP-optical emission spectrometer (ICP-OES) using Yt and Au as internal standards. Certified reference materials (CRM) were run to check for precision and accuracy. The reproducibility of the SLRS-3 water standard was <4% (%RSD) for both Ba and Ca and mean values were within 5% of the recommended values for both elements (*n* = 8). Phytoplankton pigments were analyzed at NIOO-CEME, Yerseke, NL, using reverse-phase HPLC (see Gieskes et al., 1988) with a reproducibility of 2.7% (or 0.3 µg/L; 1σ) for Chl a, based on an in-house standard (*n* = 7). Hemolymph samples were defrosted and 150 µl of sample was pipetted into a clean Teflon beaker. The sample was digested by adding 150 µl HNO$_3$ and 150 µl H$_2$O$_2$ (trace metal grade) and allowing the reaction to take place in the sealed beaker at 60 °C for more than 12 h. In and Re

were used as internal standards to control instrument fluctuations. Samples were analyzed for Ba and Ca on a Finnigan Element2 High Resolution-Inductively Coupled Plasma-Mass Spectrometer (HR-ICP-MS). Samples were diluted 20 times with deionized water (>18 MΩ/cm) to assure a salt concentration less than 0.2%. Reproducibility of seawater and hemolymph samples was <5% for both Ba and Ca ([Ba/Ca]$_{hemolymph}$ = 3.8 ± 0.2 µmol/mol, *n* = 9, and [Ba/Ca]$_{water}$ = 65.1 ± 2.1 µmol/mol, *n* = 9).

Three animals from each laboratory treatment were randomly selected and their tissues were digested following the protocol of Blust et al. (1988). Briefly, samples were digested in 2 ml of bi-distilled HNO$_3$ for at least 12 h and were then microwave digested with the addition of 1 ml of Ultrapure H$_2$O$_2$. The digested tissue samples were then analyzed for Ba and Ca with the HR-ICP-MS in the same manner as hemolymph (see above). Reproducibility was established by running different CRMs, the DORM-2 Dogfish muscle (National Research Council of Canada) and the NIST 1566a oyster tissue. For DORM-2, reproducibility was 4.8% ([Ba/Ca] = 1.16 ± 0.05 mmol/mol, *n* = 5), while it was 7.6% for 1566a oyster tissue ([Ba/Ca] = 0.22 ± 0.02 mmol/mol, *n* = 7). Neither of these CRMs are certified for Ba concentrations, but values obtained for NIST 1566a were within 10% of previously published values (see Buckel et al., 2004).

Shells were sectioned along the axis of maximal growth using a wet diamond saw. Thick sections were viewed under an optical microscope with UV light and calcein marks were mapped for each shell. Only shells from the laboratory experiments with greater than 70 µm of new growth were used (the laser ablation spot is 50 µm in diameter, see further). Unfortunately, mussels from the feeding experiment were not exposed to calcein for a long enough period (4 h). Therefore, the new growth could not be assessed and these shells could not be analyzed for Ba/Ca ratios. Shells from the field experiment were first sampled for stable isotopes. Carbonate powder was milled from the shell cross-sections using a 300 µm drill bit and a Merchantek Micromill (a fixed drill and computer controlled micro positioning device), which allows precise sampling. Samples were milled from the outer calcite shell layer. Various sampling distances were used (150 µm to 1 mm) depending on growth rate (i.e., fewer samples in regions of high growth). Oxygen and carbon isotope analyses were performed using a ThermoFinnigan Kiel III coupled to a ThermoFinnigan Delta+XL dual inlet isotope ratio mass spectrometer (IRMS). The samples were calibrated against the NBS-19 standard ($\delta^{18}O$ = −2.20‰, $\delta^{13}C$ = +1.95‰) and data are reported as ‰ VPDB using the conventional delta notation. The reproducibility (1σ) of the routinely analyzed carbonate standard is better than 0.1‰ for both $\delta^{18}O$ and $\delta^{13}C$ (more details can be found in Gillikin et al., 2005b). High resolution Ba/Ca profiles from field grown shells were obtained using either solution nebulization HR-ICP-MS (SN-HR-ICP-MS) on micromilled powders (powders were milled directly beneath the isotope sample to assure proper

alignment of the data and to remove surface contamination) or by laser ablation ICP-MS (LA-ICP-MS; see below). All shells from the dissolved Ba experiment with adequate growth were analyzed for Ba/Ca using the LA-ICP-MS.

Carbonate powders for Ba/Ca analyses ($\sim$150 µg) were dissolved in a 1 ml of 5% HNO_3 solution containing 1 ppb of In and Re, which were used as internal standards. Reproducibility of Ba/Ca ratios over the sampling period was 6.6% (1σ; or 0.06 µmol/mol) based on replicate measurements of a *M. edulis* in-house reference material ([Ba/Ca] = 0.96 µmol/mol; $n = 8$). Accuracy was assessed using the USGS MACS1 carbonate standard ([Ba/Ca] = 84.76 µmol/mol) and was found to be within 1% of the recommended value ($n = 6$; values from S. Wilson, USGS, unpublished data, 2004).

Data from LA-ICP-MS were calibrated using both the NIST 610 (values from Pearce et al. (1997)) and the USGS MACS1 (values from S. Wilson, USGS, unpublished data, 2004). The laser was shot ($\sim$50 µm spots) directly in the holes of the isotope sampling allowing direct alignment of Ba/Ca and isotope profiles for the field experiment (cf. Toland et al., 2000). All shells from the laboratory experiment were analyzed in front of the calcein mark (one analysis per shell, if growth was less than 50 µm, the shell was not sampled). Calibration (including gas blank subtraction, ^{43}Ca normalization, and drift correction) was performed offline following Toland et al. (2000). Ba/Ca reproducibility over the sampling period was 0.11 µmol/mol (1σ; or 12.8%) at the 1 µg/g level (MACS2, mean = 0.9 µmol/mol, $n = 17$) and 5.9 µmol/mol (1σ; or 7.3%) at the 80 µg/g level (MACS1, mean = 80.5 µmol/mol, $n = 47$), which covers the full range of Ba/Ca values encountered in this study (see Section 3). Accuracy was assessed using MACS2; as there is no recommended value available for MACS2, we used our own SN-HR-ICP-MS data (MACS2 = 0.90 ± 0.07 µmol/mol $n = 5$), which indicate a robust LA-ICP-MS calibration. Details of operating conditions can be found in Lazareth et al. (2003). Briefly, the system consists of a Fisons-VG frequency quadrupled Nd-YAG laser (266 nm) coupled to a Fisons-VG Plasma-Quad II+ mass spectrometer.

The background or baseline [Ba/Ca]$_{shell}$ was selected by first omitting obvious peaks (e.g., $\sim$15–22 mm from the umbo in shell KN200203), then omitting all data that was greater than 50% of the (peak-less) mean. This was repeated until the change in mean [Ba/Ca]$_{shell}$ was less than 5%. This provided an objective criterion for selecting background [Ba/Ca]$_{shell}$ data.

3. Results

3.1. Laboratory experiments

3.1.1. Hemolymph

In the dissolved Ba experiment, *M. edulis* [Ba/Ca]$_{hemolymph}$ was only slightly different from the [Ba/Ca]$_{water}$, with the linear least squares regression
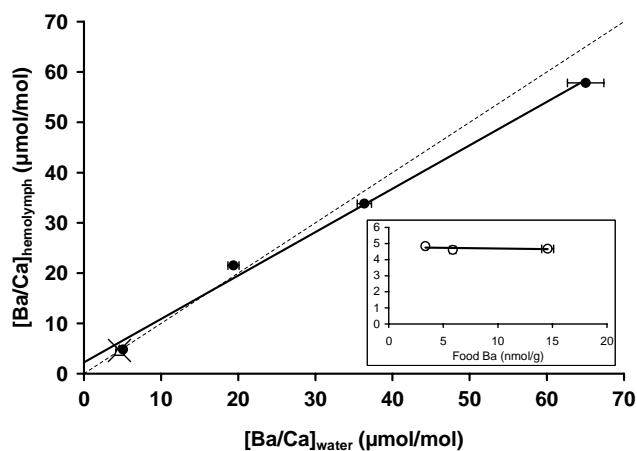

Fig. 2. Mean Ba/Ca ratios (±SE) in hemolymph of laboratory grown *M. edulis* versus Ba/Ca ratios of culturing water (±SE; solid circles). Some error bars are smaller than the symbols. The solid line shows the linear least squares regression, with the relationship [Ba/Ca]$_{hemolymph}$ = 0.86 (±0.04) × [Ba/Ca]$_{water}$ + 2.26 (±1.49) ($R^2 = 0.98$, $p < 0.0001$, $n = 36$ in four treatments). The 1:1 line is also shown (dashed). Data from the feeding experiment, where the mussels were fed food enriched in Ba are shown as the X and diamond. The inset graph illustrates that food [Ba] does not influence hemolymph Ba/Ca ratios (*y*-axis legend is the same as the main graph).

$$[\text{Ba/Ca}]_{hemolymph} = 0.86(\pm 0.04) \times [\text{Ba/Ca}]_{water} + 2.26(\pm 1.49) \tag{1}$$

(in µmol/mol; $R^2 = 0.98$, $p < 0.0001$, $n = 36$, in four treatments) (Fig. 2, Table EA1). The errors of the regression coefficients reported above (and hereafter) represent the 95% confidence intervals (95% CI), and are based on among individual variation and not among treatment variation. Despite the Ba difference in foods offered (3.35, 5.87, and 14.56 nmol/g DW Ba), hemolymph was similar between the three treatments of the feeding experiment (Fig. 2, inset; Table EA1).

3.1.2. Tissues

In the dissolved Ba experiment, tissue Ba/Ca was slightly enriched as compared to [Ba/Ca]$_{water}$ in the ambient treatment but was reduced by almost half in the highest [Ba/Ca]$_{water}$ treatment (Fig. 3). This resulted in an exponential fit between water and tissue

$$[\text{Ba/Ca}]_{tissue} = 35.36(\pm 2.19) \times (1 - \exp\{(-0.07(\pm 0.01) \times [\text{Ba/Ca}]water)\}) \tag{2}$$

(in µmol/mol; $R^2 = 0.99$, $p < 0.0001$, $n = 11$, in four treatments) (Fig. 3, Table EA1). Although we do not have enough data for statistics, it is clear that there is a trend of increasing tissue Ba/Ca with increasing food Ba (Fig. 3, inset; Table EA1) in the feeding experiment.

3.1.3. Shells

Between six and nine shells were analyzed for each Ba treatment (see Table EA1). In the dissolved Ba experiment, [Ba/Ca]$_{shell}$ was directly proportional to [Ba/Ca]$_{water}$ with the linear relationship
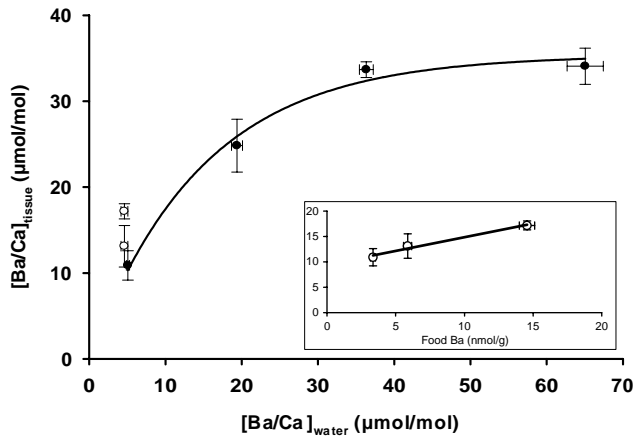
Fig. 3. Mean Ba/Ca ratios (±SE) in bulk tissue of laboratory grown *M. edulis* versus Ba/Ca ratios of culturing water (±SE; solid circles). Some error bars are smaller than the symbols. The solid line shows the exponential fit, with the relationship $[Ba/Ca]_{tissue} = 35.36 \ (\pm 2.19) \times (1 - \exp\{(-0.07(\pm 0.01) \times [Ba/Ca]water)\})$ $(R^2 = 0.99, \ p < 0.0001, \ n = 11$ in four treatments). Data from the feeding experiment, where the mussels were fed food enriched in Ba are shown as the open symbols. The inset graph illustrates that food [Ba] clearly does influence tissue Ba/Ca ratios (*y*-axis legend is the same as the main graph).

$$[Ba/Ca]_{shell} = 0.10 (\pm 0.02) \times [Ba/Ca]_{water} + 1.00 (\pm 0.68)$$

(3)

(in µmol/mol; $R^2 = 0.84$, $p < 0.0001$, $n = 28$, in four treatments) (Fig. 4, Table EA1). To calculate the partition coefficient (D_{Ba}), many studies force the regression through zero (see Lea and Spero, 1992; Zacherl et al., 2003); yet, considering that our intercept is well above zero, we chose not to force through the origin, resulting in a D_{Ba} of 0.10 ± 0.02 (95% CI). However, it should be noted here that forcing through the origin does not significantly change the D_{Ba} (0.12 ± 0.01; 95% CI) (*t* test, $p = 0.38$).
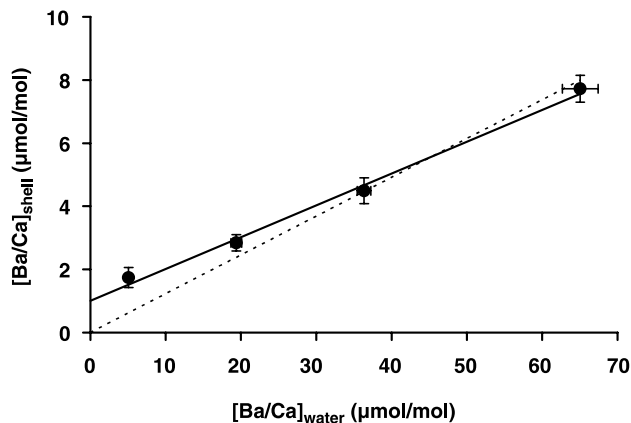

Fig. 4. Mean Ba/Ca ratios (±SE) in shells of laboratory grown *M. edulis* versus Ba/Ca ratios of culturing water (±SE). Some error bars are smaller than the symbols. The solid line shows the linear least squares regression, with the relationship $[Ba/Ca]_{shell} = 0.10 \ (\pm 0.02) \times [Ba/Ca]_{water} + 1.00 \ (\pm 0.68)$ $(R^2 = 0.84, \ p < 0.0001, \ n = 28$ in four treatments). The dashed line represents the regression forced through zero.

Although shells were collected in early March, prior to the onset of the spring phytoplankton bloom (see further) and formation of the shell Ba/Ca peak, we analyzed a few shells just behind the calcein mark to assess if the shells were collected during the formation of a 'Ba/Ca peak,' but these shell regions did not exhibit elevated $[Ba/Ca]_{shell}$ indicative of the Ba/Ca peak.

3.2. Field experiment

3.2.1. Environmental parameters

All four sites had significantly different salinity and $[Ba/Ca]_{water}$ values (Figs. 5A and B; ANOVA, $p < 0.0001$; post hoc LSD test, all $p < 0.01$; Table EA2) and there was a

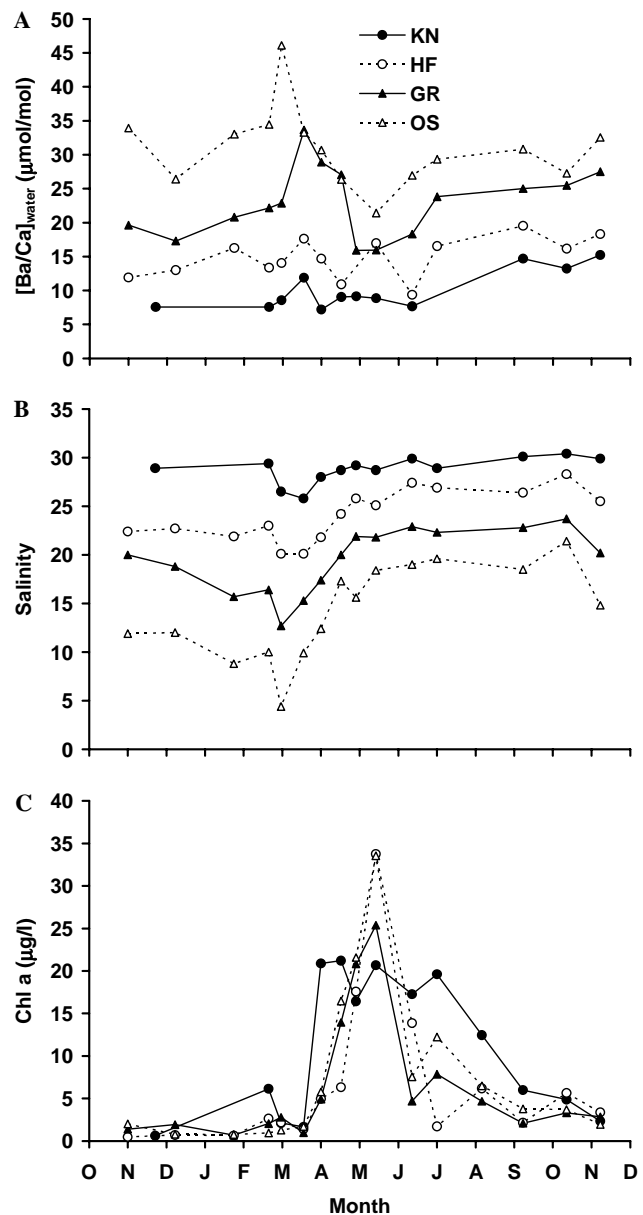Fig. 5. Dissolved $[Ba/Ca]_{water}$ (A), salinity (B), and Chl *a* (C) at the four Schelde sites measured over one year (November 2001–November 2002). See Fig. 1 for site abbreviations.
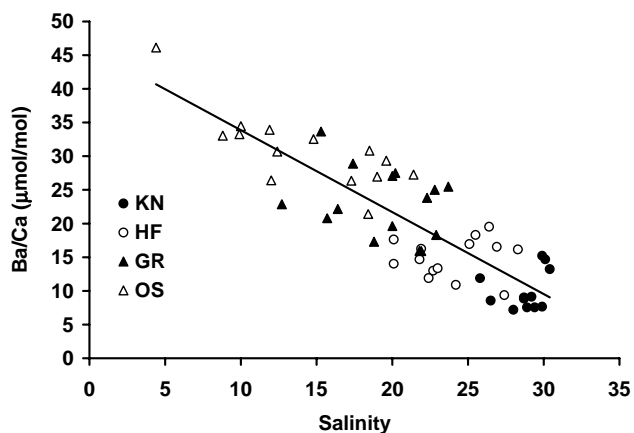
Fig. 6. Salinity versus $[Ba/Ca]_{water}$, including data from all sites and sampling dates, with the linear relationship $[Ba/Ca]_{water} = -1.22$ $(\pm 0.21) \times$ Salinity $+ 46.05$ (± 4.57) $(R^2 = 0.73, n = 55, p < 0.0001)$. See Fig. 1 for site abbreviations.

highly significant negative relationship between $[Ba/Ca]_{water}$ and salinity (Fig. 6; in μmol/mol; $R^2 = 0.73$, $n = 55$, $p < 0.0001$) with the linear relationship

$$[Ba/Ca]_{water} = -1.22(\pm 0.21) \times \text{Salinity} + 46.05(\pm 4.57).$$
(4)

The large scatter in these data is undoubtedly due to changes in the effective river end member as was previously demonstrated for the Schelde estuary (Coffey et al., 1997). There was no overall difference between Chl a concentrations at any of the stations (ANOVA, $p = 0.43$), with the phytoplankton bloom starting in April and ending in late summer at all sites (Fig. 5C). The temperature profiles from the four sites were remarkably similar, with an annual range of 0–20 °C (data not shown).

3.2.2. Shells

For the six shells analyzed, $\delta^{18}O$, $\delta^{13}C$, and $[Ba/Ca]_{shell}$ profiles are plotted against distance from the umbo in Fig. 7. All profiles are characterized by the typical low level background $[Ba/Ca]_{shell}$, interrupted by sharp episodic peaks (aside from one shell from OS, Fig. 7). Using the inverted $\delta^{18}O$ scale as a temperature and season indicator (i.e., positive $\delta^{18}O$ in winter), it is clear that these Ba peaks in the shell occur during spring when SST started to rise. The two shells which were transplanted from the Oosterschelde (sites HF and GR) showed clear calcein marks in their shells, which coincided with abrupt changes in the stable isotope profiles. The change in the $\delta^{13}C$ profile is most pronounced in the GR shell as this site has a much lower salinity (Fig. 5B) and hence a more negative $\delta^{13}C$ of dissolved inorganic carbon (DIC), compared to the Oosterschelde, where these animals were collected.

After selecting only the background $[Ba/Ca]_{shell}$ data from the shells (filled circles in Fig. 7, Table EA2), there was a highly significant linear relationship between

background $[Ba/Ca]_{shell}$ and average $[Ba/Ca]_{water}$ data from the whole year:

$$\text{background}[Ba/Ca]_{shell} = 0.071(\pm 0.001) \times [Ba/Ca]_{water}$$
(5)

(in μmol/mol; $R^2 = 0.96$, $p < 0.0001$, $n = 233$ [data of six shells from four sites]). As opposed to the laboratory data, these data do include zero in the intercept, which was found to be not significant ($p = 0.79$; 95% CI range $= -0.16$ to $+0.12$) and was therefore not included in the regression. Thus, the D_{Ba} determined from the field experiment is 0.071 (± 0.001), which is significantly different from the D_{Ba} determined in the laboratory (Fig. 8; t test, $p < 0.001$).

4. Discussion

4.1. Pathway of barium incorporation into the shell

Biomineralization in bivalves takes place in the extrapallial fluid (EPF), a thin film of liquid between the calcifying shell surface and the mantle epithelium (Wheeler, 1992). The central EPF is where the inner aragonite shell layer is precipitated, whereas the outer calcite shell layer is precipitated from the marginal EPF (i.e., the layer analyzed in this study). The EPF is isolated from seawater and therefore may have different elemental concentrations than seawater. Although there are numerous reports on central EPF elemental concentrations (e.g., Crenshaw, 1972; Wada and Fujinuki, 1976), direct measurements of the marginal EPF are difficult and we know of only one report providing marginal EPF elemental concentrations (Lorens, 1978), but unfortunately Ba was not measured. However, there does not seem to be a difference in Ba concentrations between hemolymph and central EPF in other bivalve species (A. Lorrain, unpublished data).

Elements move into the EPF through the epithelial mantle cells which are supplied from the hemolymph (Wilbur and Saleuddin, 1983). Ions enter the hemolymph of marine mollusks primarily through the gills, although they may also enter via the gut (see Wilbur and Saleuddin, 1983, and references therein). The relative contributions of Ba to the shell from food versus environment are unknown; however, mollusk guts are known to contain high Ba concentrations (Lobel et al., 1991; A. Lorrain, unpublished data). Therefore, it is possible that the gut is a source of Ba in mollusk shells. However, if food Ba impacted background $[Ba/Ca]_{shell}$, the regression between background $[Ba/Ca]_{shell}$ and $[Ba/Ca]_{water}$ would not go through zero (meaning zero $[Ba/Ca]_{water} =$ zero $[Ba/Ca]_{shell}$). In the field specimens, the regression does go through zero (Fig. 8). This, together with the good correlation with $[Ba/Ca]_{water}$, makes it very unlikely that food is a major source of Ba to the shell during those times when background $[Ba/Ca]_{shell}$ is observed. Nevertheless ingested particulate Ba may be involved in the formation of the $[Ba/Ca]_{shell}$ peaks (see Section 4.3).
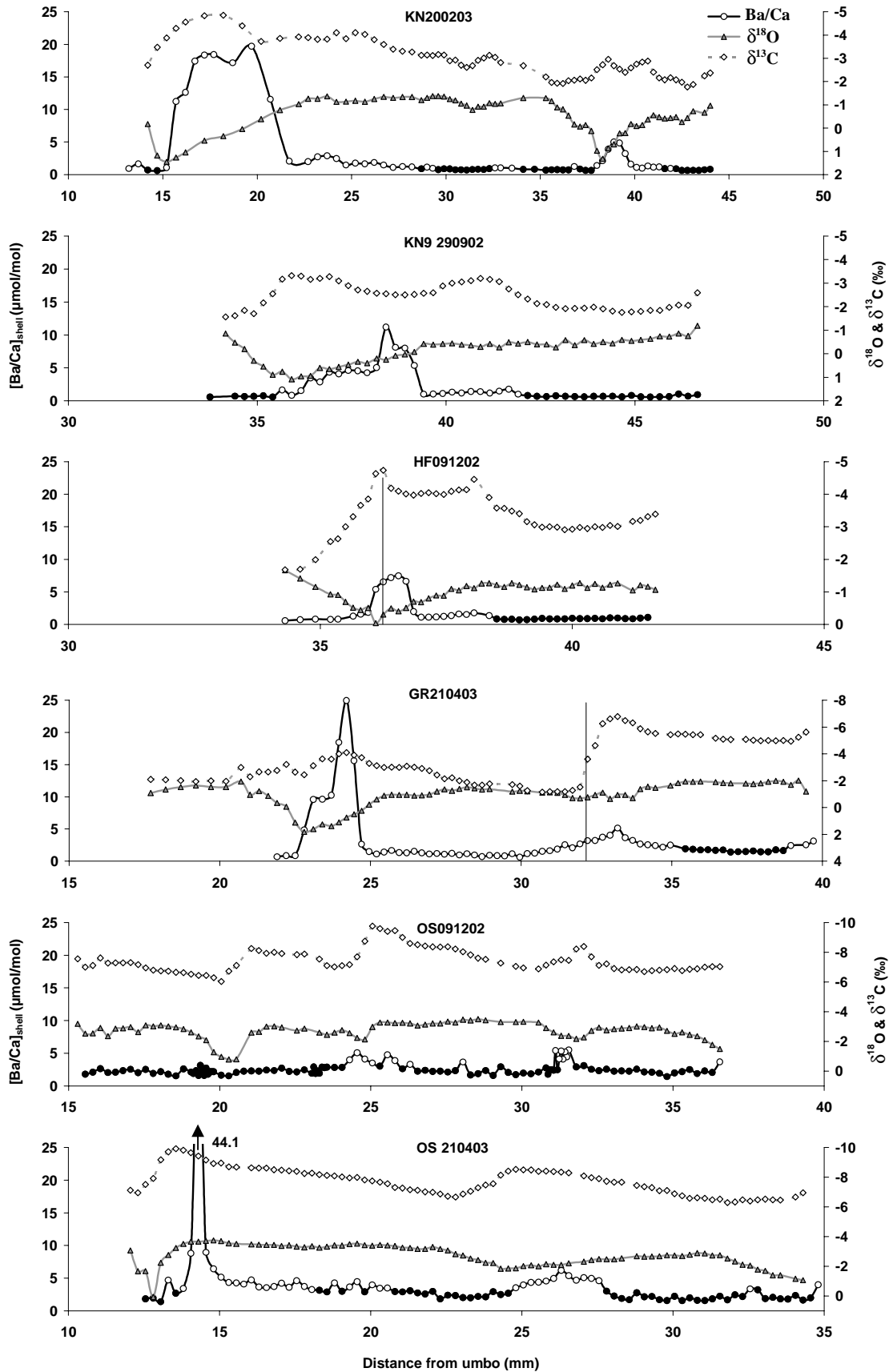
Fig. 7. High resolution $\delta^{18}O$, $\delta^{13}C$, and [Ba/Ca]$_{shell}$ profiles from the six shells. Black filled symbols denote data selected as background [Ba/Ca]$_{shell}$ data. Vertical lines correspond to the time of transplantation (HF and GR shells only, see Section 2) as determined from the calcein stain. Shell codes represent collection site and date (format: ddmmyy). Note that the isotope axes are inverted.
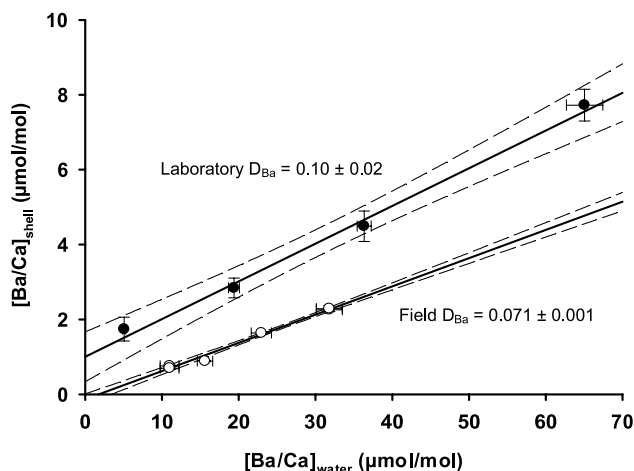
Fig. 8. Mean [Ba/Ca]$_{shell}$ ($\pm$SE) in shells of laboratory grown (closed symbols; based on 28 shells from four treatments) and field grown (open symbols; based on multiple data from six shells from four sites, background data only) *M. edulis* versus Ba/Ca ratios of water ($\pm$SE). The average [Ba/Ca]$_{water}$ over the whole year is used for the field regression (see text, Section 4.2). The solid line shows the linear least squares regressions and the dashed lines the 95% CI. Slopes are significantly different (*t* test) at $p < 0.0001$.

4.2. *Mytilus edulis calcite* D_{Ba}

Both the laboratory and field experiments verify that there is a direct relationship between background [Ba/Ca]$_{shell}$ and [Ba/Ca]$_{water}$ in *M. edulis* calcite. A possible reason for the difference in slopes between the laboratory and field experiment [Ba/Ca]$_{shell}$ vs. [Ba/Ca]$_{water}$ (Fig. 8) may be that we did not replicate treatments in the laboratory, but only individuals within a treatment, while we had an overall low number of samples form the field experiment. An alternative explanation could be that the stress of handling and the suddenly increased Ba concentration in the laboratory experiments caused a saturation of the ionoregulatory ability of the animal. Lorens and Bender (1980) found that elemental ratios in shells increased in laboratory held *M. edulis* for a short while, then decreased (they termed this section of the shell "transition zone calcite" (or TZC)). They proposed that this was caused by the stress of capture and the adjustment to a new environment. Although we acclimated these animals to laboratory conditions for 3 weeks, the change to the experimental conditions may have caused stress and we may have included TZC in our analyses. This could explain the higher D_{Ba} in the laboratory cultured mussels. Furthermore, the fact that the regression does not go through the origin supports this. As in the field population, it can be expected that when there is zero Ba in the water, there should be zero Ba in the shell. Interestingly, as the hemolymph can be expected to represent the crystallization fluid better than seawater, when a regression between hemolymph and shell is performed (laboratory experiment), the regression does go through the origin (intercept not significant, $p = 0.07$). The D_{Ba} calculated using hemolymph, 0.134 ($\pm$0.006) ($R^2 = 0.95$, $n = 25$,

$p < 0.0001$), is also more similar to that for planktonic foraminifera (see further).

Alternatively, the field D_{Ba} may also not be accurate, we averaged the [Ba/Ca]$_{water}$ from the whole year, while it is clear that the background [Ba/Ca]$_{shell}$ is formed from approximately mid-summer to the end of the growing season. Selecting only the [Ba/Ca]$_{water}$ from July to November changes the regression slightly, but significantly to background [Ba/Ca]$_{shell} = 0.091$ ($\pm$0.006) $\times$ [Ba/Ca]$_{water} - 0.52$ ($\pm$0.17) ($R^2 = 0.76$, $p < 0.0001$), and when only selecting September to November it changes to background [Ba/Ca]$_{shell} = 0.081$ ($\pm$0.006) $\times$ [Ba/Ca]$_{water} - 0.26$ ($\pm$0.15) ($R^2 = 0.76$, $p < 0.0001$). Therefore, considering both the laboratory and field data, we propose that the D_{Ba} for *M. edulis* lies within the range of 0.07–0.12. Furthermore, the algorithm used to select the background [Ba/Ca]$_{shell}$ data used here may be excluding some [Ba/Ca]$_{water}$ data stored in the shell. It is possible that all [Ba/Ca]$_{shell}$ data between large [Ba/Ca]$_{shell}$ peaks are recording [Ba/Ca]$_{water}$. If this was the case, seasonal [Ba/Ca]$_{water}$ could be reconstructed; however, this could only be determined from more detailed experiments. Nevertheless, these data do illustrate that average [Ba/Ca]$_{water}$ can be estimated from *M. edulis* shells using the proposed algorithm to select the background [Ba/Ca]$_{shell}$ data.

It should be noted that incorporation of elements in calcite with ionic radii larger than calcium (such as Ba) are expected to be strongly affected by external factors, such as temperature or salinity (Pingitore and Eastman, 1984; Morse and Bender, 1990). We are unable to determine if salinity has an effect or not. The strong relationship in the field between [Ba/Ca]$_{water}$ and salinity makes it difficult to deconvolve the effects, whereas in the laboratory salinity was similar in all treatments. Therefore, this could be another reason for the difference in intercepts between the two experiments. Considering the seasonal 20 °C temperature range at these sites (from $\sim$0 to 20 °C), and the stable background [Ba/Ca] ratios observed in these shells, it does not seem likely that there is a major temperature effect on background D_{Ba} in *M. edulis*. This is most probably true for all bivalves as well, as the stable Ba background in all published data is evident and temperature almost always has a seasonal cyclicity. Similarly, Lea and Spero (1994) did not find an influence of temperature on D_{Ba} in foraminifera, and no temperature effect has been reported for inorganic calcite. However, definitive experiments should be carried out to confirm that temperature does not affect bivalve background [Ba/Ca] ratios.

Abiogenic experiments on the D_{Ba} in calcite have provided a range of values, which is probably due to unconstrained precipitation rates in many of the experiments (Tesoriero and Pankow, 1996). For the range of *M. edulis* shell precipitation rates estimated by Lorens (1981), D_{Ba} is expected to range between 0.03 and 0.05 according to the abiogenic calcite experiments of Tesoriero and Pankow (1996). Pingitore and Eastman (1984) provided an inorganic D_{Ba} of 0.06 ± 0.01, which is very similar to the low end

of the range we estimate for *M. edulis* D_{Ba} (i.e., 0.07). Planktonic foraminifera, on the other hand can have higher D_{Ba} than *M. edulis*, ranging from 0.09 to 0.19 (Lea and Boyle, 1991; Lea and Spero, 1992, 1994), whereas benthic foraminifera have an even higher D_{Ba} in both laboratory (0.2–0.5; Havach et al., 2001) and field based studies (0.37; Lea and Boyle, 1989). It can generally be considered that when the partition coefficient of a particular element (D_{Me}) is far from inorganically determined D_{Me}, then other factors most likely influence D_{Me}, such as the physiology of the organism or other biological factors. For example, Sr/Ca in corals has been shown to be a good SST proxy and the D_{Sr} is close to one (Weber, 1973), which is similar to abiogenic aragonite (Kinsman and Holland, 1969), whereas in aragonitic bivalve shells the D_{Sr} is around 0.25 and there is no link with SST (Gillikin et al., 2005a). The fact that foraminiferal Ba/Ca has successfully been used as a proxy of dissolved Ba/Ca, and that the foraminiferal D_{Ba} is farther from expected values than *M. edulis*, further implies that Ba/Ca in *M. edulis* has great potential as a robust proxy of dissolved seawater Ba/Ca, as there should be an even smaller biological effect in *M. edulis* calcite.

To test this proxy further, we use data from shell GR210403 for the period preceding transplantation. These data should be representative of Oosterschelde conditions with salinity above 30 (see Section 2.2). The background [Ba/Ca]$_{shell}$ before transplantation is 0.98 ± 0.05 ($n = 13$), which corresponds to a [Ba/Ca]$_{water}$ of 13.8 ± 0.7 when using a D_{Ba} of 0.07 and 8.2 ± 0.4 when using a D_{Ba} of 0.12. A range of [Ba/Ca]$_{water}$ of 8–14 is reasonable for a salinity of about 30 (Fig. 6) and provides additional evidence that even at low [Ba/Ca]$_{water}$, this is a good proxy.

4.3. High resolution barium profiles

Our results confirm the general Ba profiles recorded in other bivalves (e.g., Stecher et al., 1996; Toland et al., 2000; Vander Putten et al., 2000; Torres et al., 2001; Lorrain, 2002; Lazareth et al., 2003; Gillikin, 2005), with a stable background signal interrupted by sharp episodic peaks, generally occurring in the spring (using $\delta^{18}O$ as a relative temperature scale). The unstable background Ba in OS shells probably reflects the highly variable salinity at this site. Another striking feature of the profiles is that the peak amplitude seems to be correlated to the mussels' age, with younger shell sections having larger peaks. For example, shell KN200203 has a large Ba/Ca peak $\sim$20 μmol/mol at 15–22 mm of growth, while in the same shell at 38–40 mm the peak only reaches $\sim$5 μmol/mol (Fig. 7). This is reproduced in the other shells as well, with a large peak around 24 mm in shell GR210403 and small peaks around 35–40 mm in shells KN9 290902 and HF091202 (Fig. 7). This trend was also found by Vander Putten et al. (2000), who collected their *M. edulis* shells from the same estuary in 1997, suggesting that peak amplitude is not environmentally controlled. This could be an averaging effect, with the sample size integrating more growth time as shell growth

slows with age (see Goodwin et al., 2003). However, considering the width of the peaks, this does not seem probable and is more likely a physiological effect of ageing (see further).

There are several hypotheses which could explain the [Ba/Ca]$_{shell}$ peaks. The hypothesis of Stecher et al. (1996), that either Ba-rich phytoplankton or barite formed in decaying phytoplankton flocs are ingested by the filter feeding bivalve and eventually the Ba is sequestered in the shell, is plausible. However, our data do not support a direct incorporation of Ba from phytoplankton ingestion into the shell. Although we could not measure Ba in the shell in the feeding experiment, it can be assumed that ingested Ba would have to pass through the hemolymph to get to the EPF and be taken up in the shell (see Section 4.1). We fed mussels food with different Ba concentrations, which was taken up in the bulk tissues (Fig. 3, inset), but hemolymph Ba concentrations did not increase (Fig. 2, inset). However, it is possible that Ba concentrations in the food offered in this study were not high enough to have an effect (maximum $\sim$15 nmol/g). Although many marine phytoplankton species contain barium concentrations similar to that of the food used in this study, certain species can have barium concentrations as high as 420 nmol/g (dry weight; Dehairs et al., 1980) (see Fisher et al., 1991, for review). Therefore, as previously suggested by Stecher et al. (1996), the [Ba/Ca]$_{shell}$ peaks can still be related to phytoplanktonic events in some way; for example, barite ingestion (see further) or uptake of specific phytoplankton species containing high levels of barium. However, the lack of a [Ba/Ca]$_{shell}$ peak in the shell OS 091202 (Fig. 7) and the large Chl *a* peak at this site (Fig. 5C) suggest that phytoplankton blooms are not the direct cause. Nevertheless, this does not exclude barite ingestion as a cause. Indeed, invertebrates are known to directly ingest barite crystals (Brannon and Rao, 1979). It is possible that barite formation only occurs downstream from the OS site (see Stecher and Kogut, 1999), explaining the lack of a [Ba/Ca]$_{shell}$ peak at this site. This would also explain the large sharp [Ba/Ca]$_{shell}$ peak in the KN shells (Fig. 7), despite the lower broad Chl *a* peak at this site (Fig. 5C). However, particulate Ba data from the Schelde, which show a peak in the spring only at mid-salinities (Zwolsman and van Eck, 1999), do not agree with this scenario; but a more detailed sampling campaign is needed to be conclusive. Clearly, more work is needed to understand the relationship between these [Ba/Ca]$_{shell}$ peaks and phytoplankton. Therefore, further experiments for longer time periods using a larger range of [Ba] in food and possibly even barite would be useful.

An increase in [Ba/Ca]$_{water}$ is highly unlikely to be the cause of [Ba/Ca]$_{shell}$ peaks, as the 20–25 μmol/mol [Ba/Ca]$_{shell}$ peaks would require [Ba/Ca]$_{water}$ to be around 300 μmol/mol, which is clearly not the case (Fig. 5A). An alternative hypothesis may be that Ba is remobilized from tissue stores during spawning, which also occurs in the spring. Indeed, *M. edulis* tissue dry weight also exhibits

sharp episodic peaks throughout the life of the animal (Kautsky, 1982). The lack of a [Ba/Ca]$_{shell}$ peak in the OS shell could possibly be due to this mussel not spawning. Osmotic stress may have required a large part of this animals' energy budget, leaving no energy for spawning (cf. Qiu et al., 2002; Gillikin et al., 2004). It is also interesting to note that the δ^{13}C profiles coincide with changes in [Ba/Ca]$_{shell}$. This is most evident in shells KN9 290902 and HF092102, where the δ^{13}C values are more negative when the [Ba/Ca]$_{shell}$ deviates from background concentrations and are more positive when the [Ba/Ca]$_{shell}$ is at background levels (Fig. 7). Bivalve shell δ^{13}C values are known to be influenced by the incorporation of metabolically derived light carbon (i.e., ^{12}C) (McConnaughey et al., 1997). Furthermore, it has been shown that increased metabolic CO_2 production with age, relative to growth rate, leads to a larger availability of metabolic C for $CaCO_3$ precipitation and therefore results in a more negative δ^{13}C in the shell (Lorrain et al., 2004). Using this rationale, higher metabolic rates from either spawning or seasonally increased growth, caused by an increase in food supply, would also result in a more negative shell δ^{13}C. This could explain the pattern we see in these shells, and also agrees with a metabolic control on [Ba/Ca]$_{shell}$ peak amplitude as described above. However, data from the scallop, *Pecten maximus*, do not corroborate this hypothesis, with their [Ba/Ca]$_{shell}$ peaks not being correlated with spawning (Lorrain, 2002). Alternatively, the higher [Ba/Ca]$_{shell}$ could be a kinetic growth rate effect, which has been noted in inorganic calcite (Tesoriero and Pankow, 1996). Higher growth rates would also increase metabolic rates and thus lower shell δ^{13}C. Finally, it can be argued that the [Ba/Ca]$_{shell}$ peaks can be caused by higher organic matter content in the shell. Bivalve shells can contain up to 5% organic matter (see Marin and Luquet, 2004, and references therein) and Ba is known to be associated with organic matter (Lea and Boyle, 1993). However, neither Hart et al. (1997) nor Sinclair (2005) found a relationship between organic matter and Ba concentrations in other biogenic carbonates (i.e., corals), and Rosenthal and Katz (1989) suggest that Ba is bound to the crystal in mollusks. Thus it is unlikely that the Ba peaks are associated with shell regions containing higher organic content.

Remarkably, a similar phenomenon also occurs in corals, with sharp episodic Ba peaks occurring at the same time each year, which are not related to river discharge (Sinclair, 2005). However, unlike bivalves, Sinclair (2005) found that the timing of the peaks differed between coral colonies, even when they grew within 20 km of each other. The main conclusion of Sinclair (2005) regarding the cause of these peaks in corals was that there is currently no satisfactory hypothesis to explain them. This is also the case for bivalves. However, the similarities between coral and bivalve Ba/Ca peaks may suggest a common cause for these peaks. This in itself would be amazing considering the large difference in biology, ecology, and biomineralization mechanisms between these two phyla of invertebrates.

4.4. Implications for estuarine paleo-seawater chemistry

Our data suggest that *M. edulis* shells have potential as a proxy of dissolved [Ba/Ca]$_{water}$. However, it should be clear that only high resolution profiles covering an adequate amount of growth may be used to assure the correct background [Ba/Ca]$_{shell}$ is selected. This selection can also be aided using the δ^{18}O and δ^{13}C profiles. Selecting the midsummer growth region (or the most negative δ^{18}O) along with the most positive δ^{13}C should result in a good selection of background [Ba/Ca]$_{shell}$. Obviously whole shell analyses are not suitable to determine [Ba/Ca]$_{water}$, because peaks would be integrated. Once the correct background [Ba/Ca]$_{shell}$ is obtained, the [Ba/Ca]$_{water}$ may be approximated using a D_{Ba} of about 0.1. These data can be useful for giving a relative indication of salinity (different estuaries can be expected to have different salinity–[Ba/Ca]$_{water}$ relationships (Coffey et al., 1997)), which could assist with δ^{18}O interpretations (see Gillikin et al., 2005b, for more explanation). Furthermore, if [Ba/Ca]$_{water}$ was extended back through geologic time for the world's large estuaries, the overall change in the oceanic Ba budget could be better constrained. However, we stress that this proxy needs to be further refined before it should be used as a proxy of environmental conditions.

5. Summary

In both the field and laboratory we have verified that background Ba/Ca ratios in *M. edulis* shells are directly related to the Ba/Ca ratios of the water in which they grew. Our data suggest that the D_{Ba} of *M. edulis* calcite is within the range of 0.07–0.12, which is very close to the expected D_{Ba} range determined from inorganic calcite studies (0.03–0.07; Pingitore and Eastman, 1984; Tesoriero and Pankow, 1996) and is lower than foraminiferal calcite (see previous references). Although our laboratory data on the effect of Ba in food was inconclusive, they, along with data from the field, suggest that the nearly ubiquitous Ba/Ca peaks found in bivalve shells are not related to phytoplankton blooms in a simple manner, but might be related to barite ingestion. Finally, the Ba/Ca (background) proxy in bivalve shells can be used as a relative indicator of salinity, and if better constrained, can extend our knowledge of estuarine Ba cycling back through time by using fossil or archaeological shells.

Associate editor: David W. Lea

Appendix A. Supplementary data

Supplementary data associated with this article can be found in the online version at doi:10.1016/j.gca.2005.09.015.

References

Baeyens, W., van Eck, B., Lambert, C., Wollast, R., Goeyens, L., 1998. General description of the Scheldt estuary. *Hydrobiologia* **366**, 1–14.

Blust, R., Vanderlinden, A., Verheyen, E., Decleir, W., 1988. Evaluation of microwave-heating digestion and graphite-furnace atomic-absorption spectrometry with continuum source background correction for the determination of iron, copper and cadmium in brine shrimp. *J. Anal. Atom. Spectrom.* **3**, 387–393.

Brannon, A.C., Rao, K.R., 1979. Barium, strontium and calcium levels in the exoskeleton, hepatopancreas and abdominal muscle of the grass shrimp, *Palaemonetes pugio*—relation to molting and exposure to barite. *Comp. Biochem. Physiol. A—Physiol.* **63**, 261–274.

Buckel, J.A., Sharack, B.L., Zdanowicz, V.S., 2004. Effect of diet on otolith composition in *Pomatomus saltatrix*, an estuarine piscivore. *J. Fish Biol.* **64**, 1469–1484.

Carroll, J., Falkner, K.K., Brown, E.T., Moore, W.S., 1993. The role of the Ganges–Brahmaputra mixing zone in supplying barium and Ra-226 to the Bay of Bengal. *Geochim. Cosmochim. Acta* **57**, 2981–2990.

Chan, L.H., Drummond, D., Edmond, J.M., Grant, B., 1977. On the barium data from the Atlantic GEOSECS expedition. *Deep-Sea Res.* **24**, 613–649.

Coffey, M., Dehairs, F., Collette, O., Luther, G., Church, T., Jickells, T., 1997. The behaviour of dissolved barium in estuaries. *Est. Coast. Shelf Sci.* **45**, 113–121.

Crenshaw, M.A., 1972. Inorganic composition of molluscan extrapallial fluid. *Biol. Bull.* **143**, 506–512.

Dehairs, F., Baeyens, W., Goeyens, L., 1992. Accumulation of suspended barite at mesopelagic depths and export production in the Southern Ocean. *Science* **258**, 1332–1335.

Dehairs, F., Chesselet, R., Jedwab, J., 1980. Discrete suspended particles of barite and the barium cycle in the open ocean. *Earth Planet. Sci. Lett.* **49**, 528–550.

Dehairs, F., Lambert, C.E., Chesselet, R., Risler, N., 1987. The biological production of marine suspended barite and the barium cycle in the Western Mediterranean Sea. *Biogeochemistry* **4**, 119–139.

Dymond, J., Suess, E., Lyle, M., 1992. Barium in deep-sea sediment: A geochemical proxy for paleoproductivity. *Paleoceanography* **7**, 163–181.

Edmond, J.M., Boyle, E.D., Drummond, D., Grant, B., Mislick, T., 1978. Desorption of barium in the plume of the Zaire (Congo) River. *Neth. J. Sea Res.* **12**, 324–328.

Fisher, N.S., Guillard, R.R.L., Bankston, D.C., 1991. The accumulation of barium by marine-phytoplankton grown in culture. *J. Mar. Res.* **49**, 339–354.

Freitas, P., Clarke, L.J., Kennedy, H., Richardson, C., Abrantes, F., 2005. Mg/Ca, Sr/Ca, and stable-isotope ($\delta^{18}O$ and $\delta^{13}C$) ratio profiles from the fan mussel *Pinna nobilis*: Seasonal records and temperature relationships. *Geochem. Geophy. Geosys.* **6**, Q04D14. doi:10.1029/2004GC000872.

Gerringa, L.J.A., Hummel, H., Moerdijk-Poortvliet, T.C.W., 1998. Relations between free copper and salinity, dissolved and particulate organic carbon in the Oosterschelde and Westerschelde, Netherlands. *J. Sea Res.* **40**, 193–203.

Gieskes, W.W.C., Kraay, G.W., Nontji, A., Setiapennana, D., Sutomo, 1988. Monsoonal alternation of a mixed and layered structure in the phytoplankton of the euphotic zone of the Banda Sea (Indonesia), a mathematical analysis of algal pigment fingerprints. *Neth. J. Sea Res.* **22**, 123–137.

Gillikin, D.P., De Ridder, F., Ulens, H., Elskens, M., Keppens, E., Baeyens, W., Dehairs, F., 2005b. Assessing the reproducibility and reliability of estuarine bivalve shells (*Saxidomus giganteus*) for sea surface temperature reconstruction: implications for paleoclimate studies. *Palaeogeogr. Palaeoclimatol. Palaeoecol.* **228**, 70–85.

Gillikin, D.P., Lorrain, A., Navez, J., Taylor, J.W., André, L., Keppens, E., Baeyens, W., Dehairs, F., 2005a. Strong biological controls on Sr/Ca ratios in aragonitic marine bivalve shells. *Geochem. Geophy. Geosys.* **6**, Q05009. doi:10.1029/2004GC000874.

Gillikin, D.P., 2005. Geochemistry of Marine Bivalve Shells: the potential for paleoenvironmental reconstruction. *Ph.D. thesis.* Vrije Universiteit Brussel, Belgium.

Gillikin, D.P., De Wachter, B., Tack, J.F., 2004. Physiological responses of two ecologically important Kenyan mangrove crabs exposed to altered salinity regimes. *J. Exp. Mar. Biol. Ecol.* **301**, 93–109.

Goodwin, D.H., Schöne, B.R., Dettman, D.L., 2003. Resolution and fidelity of oxygen isotopes as paleotemperature proxies in bivalve mollusk shells: models and observations. *Palaios* **18**, 110–125.

Guay, C.K., Falkner, K.K., 1997. Barium as a tracer of Arctic halocline and river waters. *Deep-Sea Res. II* **44**, 1543–1569.

Guay, C.K., Falkner, K.K., 1998. A survey of dissolved barium in the estuaries of major Arctic rivers and adjacent seas. *Cont. Shelf Res.* **18**, 859–882.

Hart, S.R., Cohen, A.L., Ramsay, P., 1997. Microscale analysis of Sr/Ca and Ba/Ca in Porites. *Proceedings of the 8th International Coral Reef Symposium* **2**, 1707–1712.

Havach, S.M., Chandler, T., Wilson-Finelli, A., Shaw, T.J., 2001. Experimental determination of trace element partition coefficients in cultured benthic foraminifera. *Geochim. Cosmochim. Acta* **65**, 1277–1283.

Jacquet, S.H.M., Dehairs, F., Cardinal, D., Navez, J., Delille, B., 2005. Barium distribution across the Southern Ocean frontal system in the Crozet–Kerguelen Basin. *Mar. Chem.* **95**, 149–162.

Kautsky, N., 1982. Growth and size structure in a Baltic *Mytilus edulis* population. *Mar. Biol.* **68**, 117–133.

Kinsman, D.J.J., Holland, H.D., 1969. The co-precipitation of cations with $CaCO_3$-IV. The co-precipitation of Sr^{2+} with aragonite between 16 and 96 °C. *Geochim. Cosmochim. Acta* **33**, 1–17.

Klein, R.T., Lohmann, K.C., Thayer, C.W., 1996. Bivalve skeletons record sea-surface temperature and $\delta^{18}O$ via Mg/Ca and $^{18}O/^{16}O$ ratios. *Geology* **24**, 415–418.

Lazareth, C.E., Vander Putten, E., André, L., Dehairs, F., 2003. High-resolution trace element profiles in shells of the mangrove bivalve *Isognomon ephippium*: a record of environmental spatio-temporal variations? *Est. Coast. Shelf Sci.* **57**, 1103–1114.

Lea, D.W., Spero, H.J., 1992. Experimental determination of barium uptake in shells of the planktonic foraminifera *Orbulina universa* at 22 °C. *Geochim. Cosmochim. Acta* **56**, 2673–2680.

Lea, D.W., Spero, H.J., 1994. Assessing the reliability of paleochemical tracers: barium uptake in the shells of planktonic foraminifera. *Paleoceanography* **9**, 445–452.

Lea, D.W., 1993. Constraints on the alkalinity and circulation of glacial circumpolar deep-water from benthic foraminiferal barium. *Global Biogeochem. Cy.* **7**, 695–710.

Lea, D.W., Boyle, E., 1989. Barium content of benthic foraminifera controlled by bottom-water composition. *Nature* **338**, 751–753.

Lea, D.W., Boyle, E., 1991. Barium in planktonic foraminifera. *Geochim. Cosmochim. Acta* **55**, 3321–3331.

Lea, D.W., Boyle, E., 1993. Determination of carbonate-bound barium in foraminifera and corals by isotope dilution plasma-mass spectrometry. *Chem. Geol.* **103**, 73–84.

Lobel, P.B., Longerich, H.P., Jackson, S.E., Belkhode, S.P., 1991. A major factor contributing to the high degree of unexplained variability of some elements concentrations in biological tissue—27 elements in 5 organs of the mussel *Mytilus* as a model. *Arch. Environ. Con. Toxicol.* **21**, 118–125.

Lorens, R.B., 1978. A study of biological and physiological controls on the trace metal content of calcite and aragonite. *Ph.D. thesis*, University of Rhode Island.

Lorens, R.B., 1981. Sr, Cd, Mn and Co distribution coefficients in calcite as a function of calcite precipitation rate. *Geochim. Cosmochim. Acta* **45**, 553–561.

Lorens, R.B., Bender, M.L., 1980. The impact of solution chemistry on *Mytilus edulis* calcite and aragonite. *Geochim. Cosmochim. Acta* **44**, 1265–1278.

Lorrain, A., 2002. Utilisation de la coquille Saint-Jacques comme traceur environnemental: approches biologique et biogéochimique. *PhD thesis*, Université de Bretagne occidentale, Brest, France.

Lorrain, A., Paulet, Y.-M., Chauvaud, L., Dunbar, R., Mucciarone, D., Fontugne, M., 2004. $\delta^{13}C$ variations in scallop shells: increasing metabolic carbon contribution with body size? *Geochim. Cosmochim. Acta* **68**, 3509–3519.

Lorrain, A., Gillikin, D.P., Paulet, Y.-M., Chauvaud, L., Le Mercier, A., Navez, J., André, L., 2005. Strong kinetic effects on Sr/Ca ratios in the calcitic bivalve *Pecten maximus*. *Geology* **33**, 965–968.

Marin, F., Luquet, G., 2004. Molluscan shell proteins. *C.R. Palevol* **3**, 469–492.

McConnaughey, T.A., Burdett, J., Whelan, J.F., Paull, C.K., 1997. Carbon isotopes in biological carbonates: respiration and photosynthesis. *Geochim. Cosmochim. Acta* **61**, 611–622.

McCulloch, M., Fallon, S., Wyndham, T., Hendy, E., Lough, J., Barnes, D., 2003. Coral record of increased sediment flux to the inner Great Barrier Reef since European settlement. *Nature* **421**, 727–730.

McManus, J., Berelson, W.M., Hammond, D.E., Klinkhammer, G.P., 1999. Barium cycling in the North Pacific: implications for the utility of Ba as a paleoproductivity and paleoalkalinity proxy. *Paleoceanography* **14**, 53–61.

McManus, J., Dymond, J., Dunbar, R.B., Collier, R.W., 2002. Particulate barium fluxes in the Ross Sea. *Mar. Geol.* **184**, 1–15.

Moore, W.S., Edmond, J.M., 1984. Radium and barium in the Amazon River system. *J. Geophys. Res. Oceans* **89** (NC2), 2061–2065.

Morse, J.W., Bender, M.L., 1990. Partition-coefficients in calcite—examination of factors influencing the validity of experimental results and their application to natural systems. *Chem. Geol.* **82**, 265–277.

Paytan, A., Kastner, M., 1996. Benthic Ba fluxes in the central Equatorial Pacific, implications for the oceanic Ba cycle. *Earth Planet. Sci. Lett.* **142**, 439–450.

Pearce, N.J.G., Perkins, W.T., Westgate, J.A., Gorton, M.P., Jackson, S.E., Neal, C.R., Chenery, S.P., 1997. A compilation of new and published major and trace element data for NIST SRM 610 and NIST SRM 612 glass reference materials. *Geostand. Newsl.* **21**, 115–144.

Pingitore, N.E., Eastman, M.P., 1984. The experimental partitioning of Ba^{2+} into calcite. *Chem. Geol.* **45**, 113–120.

Purton, L.M.A., Shields, G.A., Brasier, M.D., Grime, G.W., 1999. Metabolism controls Sr/Ca ratios in fossil aragonitic mollusks. *Geology* **27**, 1083–1086.

Qiu, J.W., Tremblay, R., Bourget, E., 2002. Ontogenetic changes in hyposaline tolerance in the mussels *Mytilus edulis* and *M. trossulus*: implications for distribution. *Mar. Ecol. Prog. Ser.* **228**, 143–152.

Rosenthal, Y., Katz, A., 1989. The applicability of trace elements in freshwater shells for paleogeochemical studies. *Chem. Geol.* **78**, 65–76.

Rowley, R.J., Mackinnon, D.I., 1995. Use of the fluorescent marker calcein in biomineralisation studies of brachiopods and other marine organisms. *Bulletin de l'Institut Oceanogra phique, Monaco* **14**, 111–120.

Shaw, T.J., Moore, W.S., Kloepfer, J., Sochaski, M.A., 1998. The flux of barium to the coastal waters of the southeastern USA: the importance of submarine groundwater discharge. *Geochim. Cosmochim. Acta* **62**, 3047–3054.

Sinclair, D.J., 2005. Non river-flood barium signals in the skeletons of corals from coastal Queensland, Australia. *Earth Planet. Sci. Lett.* **237**, 354–369.

Sinclair, D.J., McCulloch, M.T., 2004. Corals record low mobile barium concentrations in the Burdekin River during the 1974 flood: evidence for limited Ba supply to rivers? *Palaeogeogr. Palaeoclimat. Palaeoecol.* **214**, 155–174.

Stecher, H.A., Kogut, M.B., 1999. Rapid barium removal in the Delaware estuary. *Geochim. Cosmochim. Acta* **63**, 1003–1012.

Stecher, H.A., Krantz, D.E., Lord, C.J., Luther, G.W., Bock, K.W., 1996. Profiles of strontium and barium in *Mercenaria mercenaria* and *Spisula solidissima* shells. *Geochim. Cosmochim. Acta* **60**, 3445–3456.

Steenmans, D., 2004. Do marine bivalve shells record paleo-productivity? *M.Sc. thesis*. Vrije Universiteit Brussel, Belgium.

Takesue, R.K., van Geen, A., 2004. Mg/Ca, Sr/Ca, and stable isotopes in modern and Holocene *Protothaca staminea* shells from a northern California coastal upwelling region. *Geochim. Cosmochim. Acta* **68**, 3845–3861.

Tesoriero, A.J., Pankow, J.F., 1996. Solid solution partitioning of Sr^{2+}, Ba^{2+}, and Cd^{2+} to calcite. *Geochim. Cosmochim. Acta* **60**, 1053–1063.

Toland, H., Perkins, B., Pearce, N., Keenan, F., Leng, M.J., 2000. A study of sclerochronology by laser ablation ICP-MS. *Ana. Atom. Spectro.* **15**, 1143–1148.

Torres, M.E., Barry, J.P., Hubbard, D.A, Suess, E., 2001. Reconstructing the history of fluid flow at cold seep sites from Ba/Ca ratios in vesicomyid clam shells. *Limnol. Oceanogr.* **46**, 1701–1708.

Tudhope, A.W., Lea, D.W., Shimmield, G.B., Chilcott, C.P., Head, S., 1996. Monsoon climate and Arabian Sea coastal upwelling recorded in massive corals from southern Oman. *Palaios* **11**, 347–361.

Vander Putten, E., Dehairs, F., Keppens, E., Baeyens, W., 2000. High resolution distribution of trace elements in the calcite shell layer of modern *Mytilus edulis*: environmental and biological controls. *Geochim. Cosmochim. Acta* **64**, 997–1011.

Wada, K., Fujinuki, T., 1976. Biomineralization in bivalve molluscs with emphasis on the chemical composition of the extrapallial fluid. In: Watabe, N., Wilbur, K.M. (Eds.), *The Mechanisms of Mineralization in the Invertebratesand Plants*. University of South Carolina Press, Columbia, pp. 175–190.

Weber, J.N., 1973. Incorporation of strontium into reef coral skeletal carbonate. *Geochim. Cosmochim. Acta* **37**, 2173–2190.

Wheeler, A.P., 1992. Mechanisms of molluscan shell formation. In: Bonucci, E. (Ed.), *Calcification in Biological Systems*. CRC press, Boca Raton, FL, pp. 179–216.

Wilbur, K.M., Saleuddin, A.S.M., 1983. Shell formation. In: Saleuddin, A.S.M., Wilbur, K.M. (Eds.), *The Mollusca*. Academic Press, New York, pp. 235–287.

Zacherl, D.C., Paradis, G., Lea, D.W., 2003. Barium and strontium uptake into larval protoconchs and statoliths of the marine neogastropod *Kelletia kelledi*. *Geochim. Cosmochim. Acta* **67**, 4091–4099.

Zwolsman, J.J.G., van Eck, G.T.M., 1999. Geochemistry of major elements and trace metals in suspended matter of the Scheldt estuary, southwest Netherlands. *Mar. Chem.* **66**, 91–111.